







Research Article

On the Design and Performance Analysis of Flexible Planar Monopole Ultra-Wideband Antennas for Wearable Wireless Applications

Deepa Thangarasu ¹, Rama Rao Thipparaju,¹ Sandeep Kumar Palaniswamy ¹,
Malathi Kanagasabai ², Mohammed Gulam Nabi Alsath ³, Devisowjanya Potti ⁴,
and Sachin Kumar ¹

¹Department of Electronics and Communication Engineering, SRM Institute of Science and Technology, Kattankulathur 603203, India

²Department of Electronics and Communication Engineering, College of Engineering, Guindy, Anna University, Chennai 600025, India

³Department of Electronics and Communication Engineering, SSN College of Engineering, Chennai 603110, India

⁴Department of Electronics and Communication Engineering, Amrita School of Engineering, Amrita Vishwa Vidyapeetham, Chennai 601103, India

Correspondence should be addressed to Sandeep Kumar Palaniswamy; vrpchs@gmail.com

Received 21 July 2022; Revised 29 August 2022; Accepted 1 September 2022; Published 26 September 2022

Academic Editor: Shobhit K. Patel

Copyright © 2022 Deepa Thangarasu et al. This is an open access article distributed under the Creative Commons Attribution License, which permits unrestricted use, distribution, and reproduction in any medium, provided the original work is properly cited.

With the promising developments in wearable communication technology, attention towards flexible electronics is increasing day-by-day. This study presents flexible low-profile ultra-wideband (UWB) antennas for wearable applications. The antenna comprised of a modified dewdrop-inspired radiator and a defected ground plane and has an impedance bandwidth of 3.1–10.6 GHz. The antenna flexibility is investigated using four different substrates (polyester, polyamide, denim, and Teslin) and tested on a cotton shirt and a high-end Res-Q jacket to evaluate their performance stability for body-worn applications. The fabricated planar dewdrop-shaped radiator (PDSR) antennas have a radiation efficiency of >90%, a gain of >4 dBi, and a group delay variation of fewer than 0.5 ns. The antenna conformability is measured by placing the fabricated antennas on various curved and nonplanar parts of the human body. The aforementioned antennas offer better flexibility for different bent conditions. The specific absorption rate (SAR) of the designed antennas is investigated to determine their wearability, and values are found to be less than 0.2 W/Kg. Also, the received signal strength (RSS) is discussed in order to analyze signal attenuation, and the performance analysis of the antennas is compared.

1. Introduction

Wearable wireless electronic systems are becoming increasingly popular around the world. Particularly, wireless body area networks (WBANs) play a significant role in sports, healthcare, and defense applications [1, 2]. An antenna is an essential element in wearable electronic transceivers for establishing effective communication among users. For the WBAN, an international standard IEEE

802.15.6 has been established to support both wideband and narrowband communications [3]. Though the standard includes various frequency bands, for research, the Industrial Scientific and Medical (ISM) band at 2.4 GHz and ultra-wideband (UWB) ranges from 3.1 to 10.6 GHz are highly preferred. Moreover, the choice of substrate is important for WBAN applications, as it should be flexible and unaffected by the aesthetic nature of human clothing. Hence, the antennas must exhibit better radiation characteristics even

TABLE 1: Properties of the flexible substrates.

Substrate	Dielectric constant (ϵ_r)	Loss tangent (δ)	Thickness (T) (mm)	Young's modulus (MPa)
Polyester	1.9	0.0045	0.99	72.9
Polyamide	3.5	0.0027	0.563	275
Denim	1.7	0.085	0.675	75.75
Teslin	2.2	0.0145	0.712	4.38

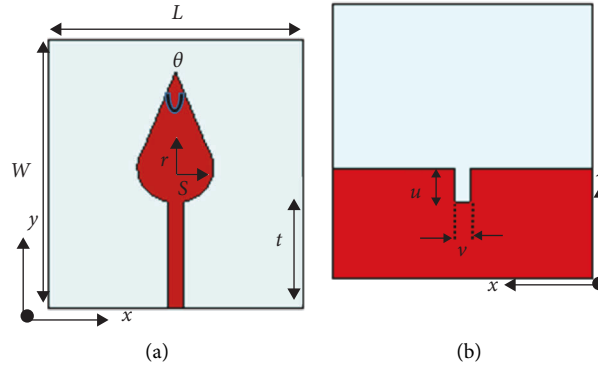


FIGURE 1: Schematic of the proposed UWB antenna: (a) front view; (b) rear view.

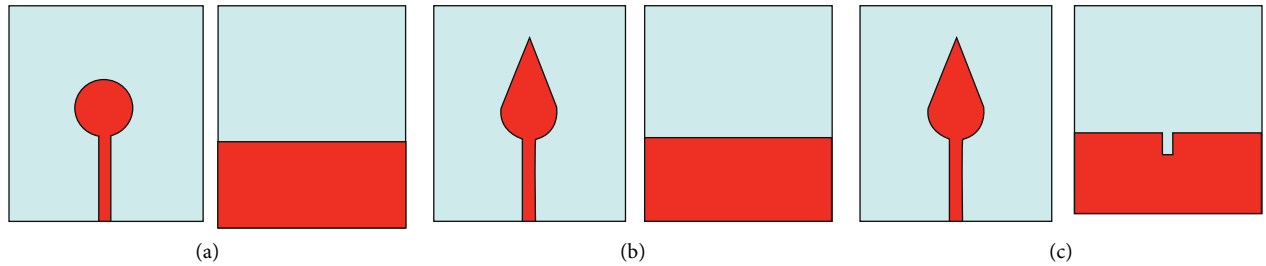


FIGURE 2: Design stages of the antenna: (a) stage 1; (b) stage 2; (c) stage 3.

under stretch/bent conditions when a human adopts different body postures. Several flexible wearable antennas have recently been reported for the ISM band [4–9]. In [4], a planar inverted-F antenna (PIFA) with an operating range of 4.96–5.9 GHz was reported for WBAN applications. In [5], a dual mode (on/off-body) antenna was presented with fabric material that resonates at 2.4 GHz for ISM application. The antennas reported in [6, 7] were designed on the FR-4 substrate and operated between 2.3 GHz and 2.6 GHz to support ISM and Bluetooth services for smartwatch applications, respectively. In [8], the radiating element is placed above the FR-4 substrate to function at 1.8 GHz for wearable applications. In [9], a patch antenna with an artificial magnetic conductor (AMC) was designed to increase gain at 2.4 GHz. In [10], a quad-band flexible antenna with a triband AMC reflector was reported for WBAN applications. Despite this, most of the reported works have less bandwidth and are large in size.

In the last decade, UWB technology has made a significant contribution to wireless communication by enabling high-speed data transfer with less interference. Due to its low power consumption, the UWB antenna is highly recommended for WBAN applications. Several

UWB antennas have been investigated in recent years using different flexible materials [11–23]. In [11], a coplanar waveguide (CPW)-fed monopole antenna with a frequency range of 7–12 GHz was designed for biomedical applications. In [12], a flexible antenna was presented with frequency selective surface (FSS) for the ISM band. In [13], a UWB antenna was presented with a flexible Kapton polyimide substrate. In [14], an elliptical monopole antenna was designed on the material Kapton and its performance was tested under crumpling conditions. In [15], a textile material was used to develop a flexible UWB antenna, and its bending and crumpling analysis was performed. In [16], a polyimide substrate was used to design a monopole antenna that covers the whole UWB range from 3.1 to 10.6 GHz. Despite this, high-cost fabrication technologies such as in-situ self-metallization were used. In [17], a semiflexible dielectric material was used to develop a circular ring-shaped UWB antenna for body-centric applications. A Y-shaped slotted antenna was reported in [18], and its performance was compared between Rogers 4350 and felt materials. A CPW-fed monopole antenna made of Kapton was reported in [19], and it was fabricated using airbrush

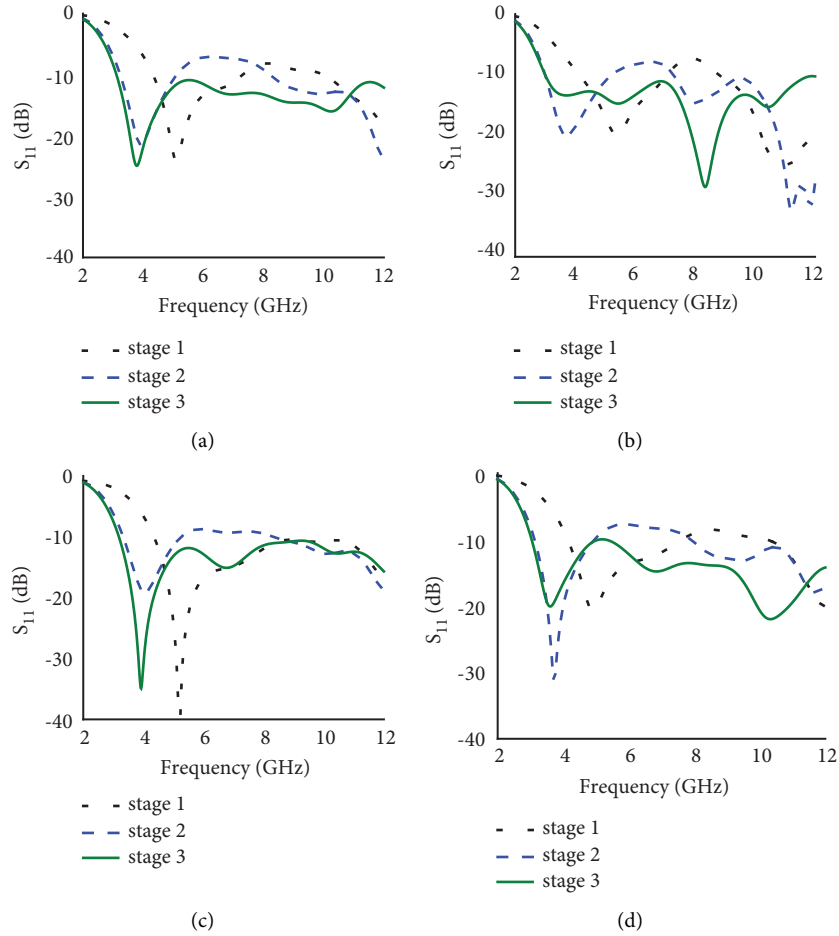


FIGURE 3: Evolution stages of the antenna using different dielectric materials: (a) polyester; (b) polyamide; (c) denim; (d) Teslin.

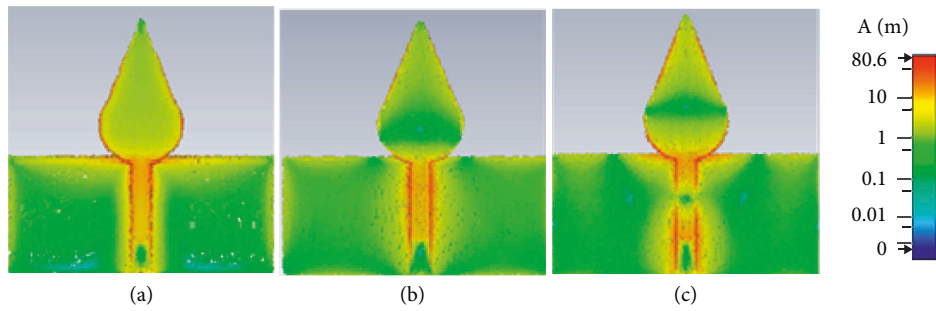


FIGURE 4: Surface current density of the UWB antenna at (a) 3.1 GHz, (b) 6.6 GHz, and (c) 10.6 GHz.

TABLE 2: Dimension of the antenna with different dielectric materials.

Substrate	Parameters							
	θ	r	s	t	w_h	w_f	u	v
Polyester				16.25	16.5	3.25	4.8	3.15
Polyamide				16	17	1	3.35	1.5
Denim	49	6	5	16	16.5	2.3	5	2.3
Teslin				16.5	17.5	2	4.1	4.1

printing technology. Although the performance of the antenna was satisfactory, its size needs to be reduced. In [20], a CPW-fed monopole antenna was designed and

backed with an EBG layer, increasing the design complexity. In [21], the antenna was supported by an AMC for the ISM band applications. In [22], a triple-band antenna

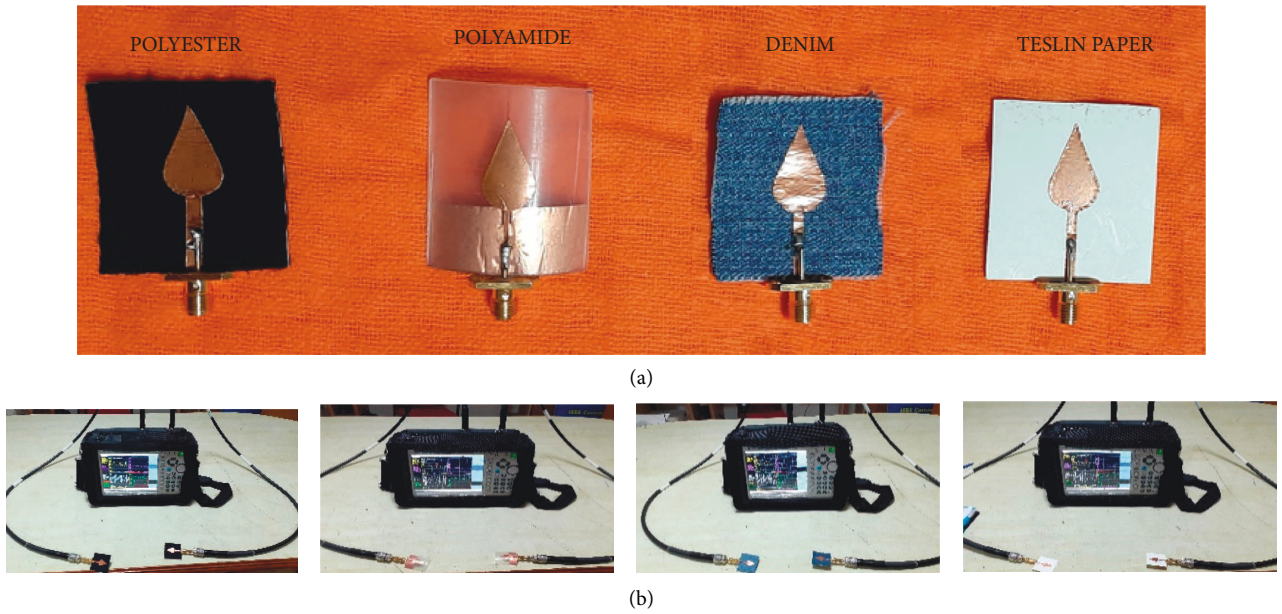


FIGURE 5: (a) Photographs of the fabricated antennas and (b) measurement photographs.

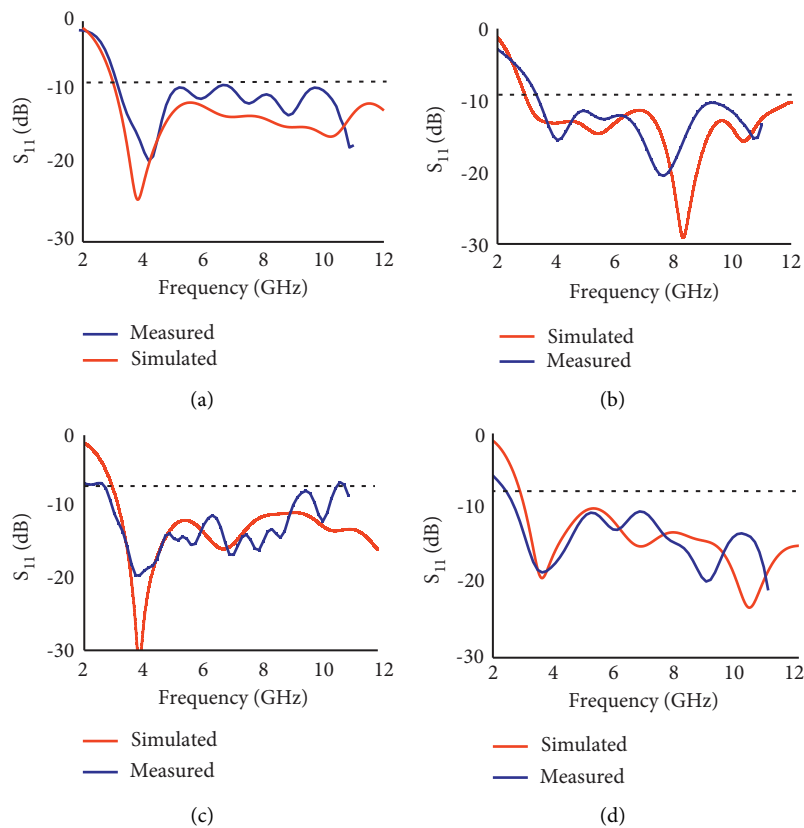
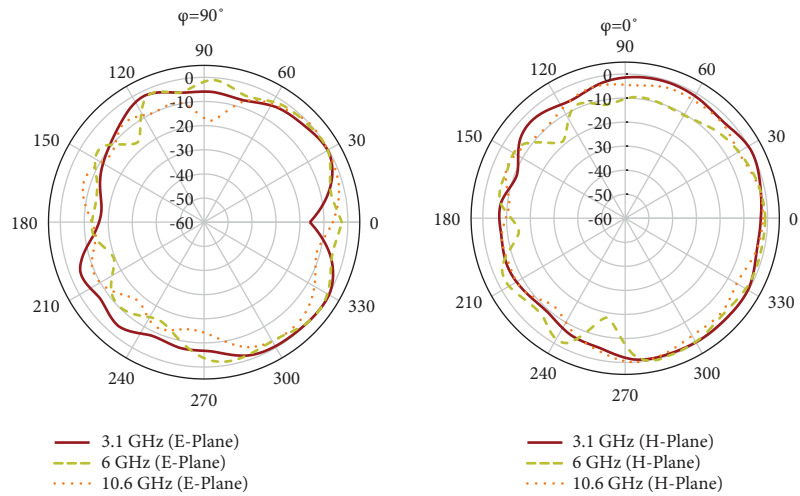


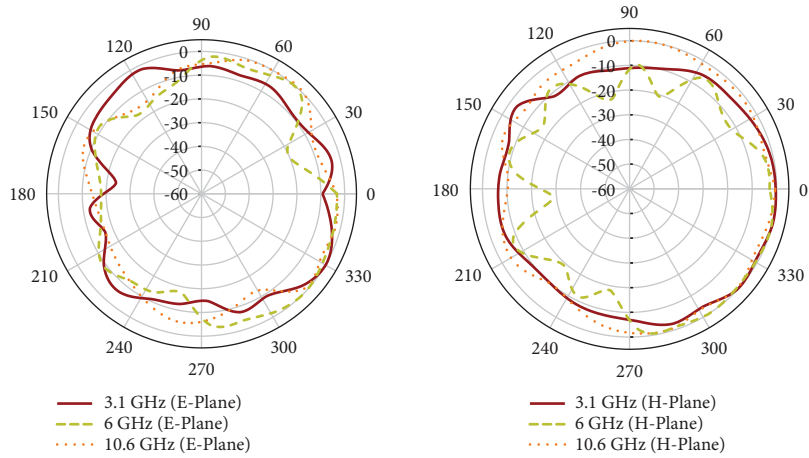
FIGURE 6: Measured and simulated S_{11} characteristics of the four antennas. (a) Polyester. (b) Polyamide. (c) Denim. (d) Teslin.

using the substrate integrated waveguide (SIW) technique was reported. In [23], a transparent flexible antenna was reported for laptop applications. In [24], an

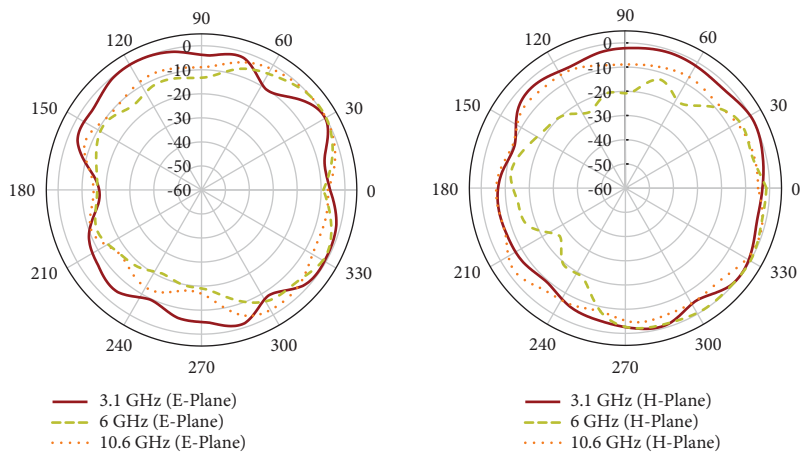
inverted-F antenna with an operating range of 0.7–1.1 GHz was demonstrated. However, most of the abovementioned antennas had design complexity, and



(a)



(b)



(c)

FIGURE 7: Continued.

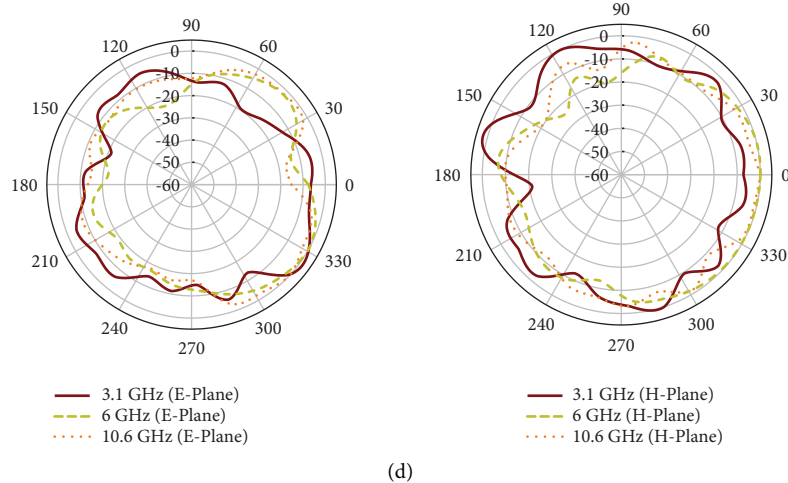


FIGURE 7: Measured radiated patterns at 3.1 GHz, 6 GHz, and 10.6 GHz. (a) Polyester. (b) Polyamide. (c) Denim. (d) Teslin.

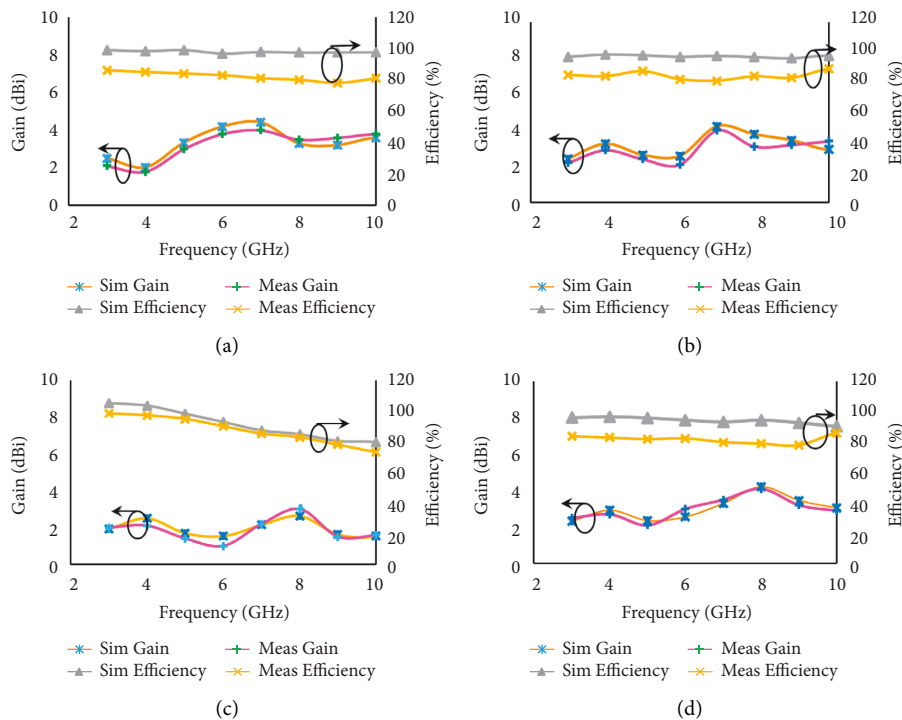


FIGURE 8: Gain and efficiency of the four antennas. (a) Polyester. (b) Polyamide. (c) Denim. (d) Teslin.

large sizes and used high-cost fabrication technology and semiflexible substrates rather than flexible substrates. Wearable antennas are now integrated into human clothing and can be used in various fields such as medicine, sports, and military to monitor patients' health, maintain body fitness and rescue soldiers in emergencies. When designing wearable antennas, several factors must be considered, such as simplicity, compactness, and flexibility to withstand bending and crumpling scenarios. The substrate should be chosen carefully so that it does not interfere with the aesthetics of

the clothing while not compromising the antenna's performance, and the specific absorption rate (SAR) must be within the acceptable range of 1.6 Watt/kg.

In this work, the aforementioned challenges are taken into account, and a simple compact flexible UWB antenna is developed using four different substrates: polyester cloth, polyamide sheet, jean cloth, and Teslin paper. Section 2 discusses the design and development of the UWB antenna, Section 3 presents the results, Section 4 illustrates the path loss analysis, and Section 5 presents the conclusion.

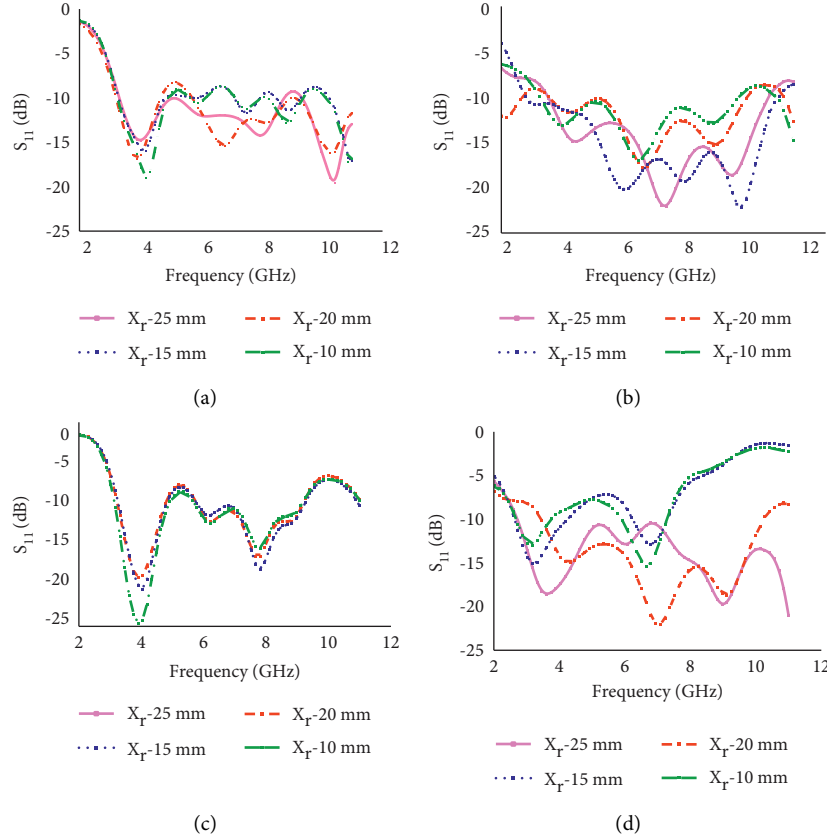


FIGURE 9: Measured reflection coefficients for different bent conditions (along the X-direction). (a) Polyester. (b) Polyamide. (c) Denim. (d) Teslin.

2. Antenna Design

The UWB antenna is developed using four different flexible substrates, and their properties are shown in Table 1. The front and rear views of the antenna are shown in Figures 1(a) and 1(b), respectively. The overall size (length \times breadth) of the antenna is 40 mm \times 42 mm.

The evolution stages of the antenna are shown in Figure 2, and the corresponding reflection coefficients on four different flexible substrates are displayed in Figure 3. In stage 1, an elliptical radiator is designed using equation (1) [25]. The elliptical-shaped radiator offers a bandwidth of 4.4–7 GHz.

$$a = \frac{F}{\{1 + 2h/\pi\epsilon_r F [\ln(\pi F/2h) + 1.7726]\}^{1/2}}, \quad (1)$$

$$\text{where } F = \frac{8.791 \times 10^9}{f_l}. \quad (2)$$

In stage 2, the electrical length of the radiator is increased by combining a triangular-shaped stub with it. This propagates the surface current to the tip of the triangular patch, resulting in a bandwidth of 3.1–10.6 GHz. The surface current distribution of the proposed antenna at 3.1 GHz, 6.6 GHz, and 10.6 GHz is shown in Figure 4. In stage 3, a slit

is etched from the ground plane, increasing the impedance bandwidth further. Finally, a planar dewdrop shaped radiator (PDSR) is proposed to achieve an impedance bandwidth of 3.1–12 GHz. The resonating frequency of the PDSR can be calculated using the following equation.

$$f_l = \frac{c}{4r \times (1 + (\pi \times \theta/360) \times \sqrt{\epsilon_{r+1}/2})}, \quad (3)$$

where r is the radius of the elliptical curved surface and θ is the angle subtended by the sides of the triangular structure. The radiator dimensions remain the same for all four antennas except for a few parameters listed in Table 2.

3. Results and Discussion

Wearable flexible electronics adhere close to the human body. Wearable devices, such as watches and safety bands, are very close to human tissues in terms of permittivity and conductivity, and thus, antenna characteristics deteriorate. Therefore, antenna performance must be measured and analyzed under various human body conditions. The antenna simulated results are evaluated using the electromagnetic (EM) computer simulation tool (CST), and the measurements are performed using the ANRITSU MS2037C vector network analyzer (VNA). Also, the bending and SAR analyses are performed. Figures 5(a) and 5(b) show

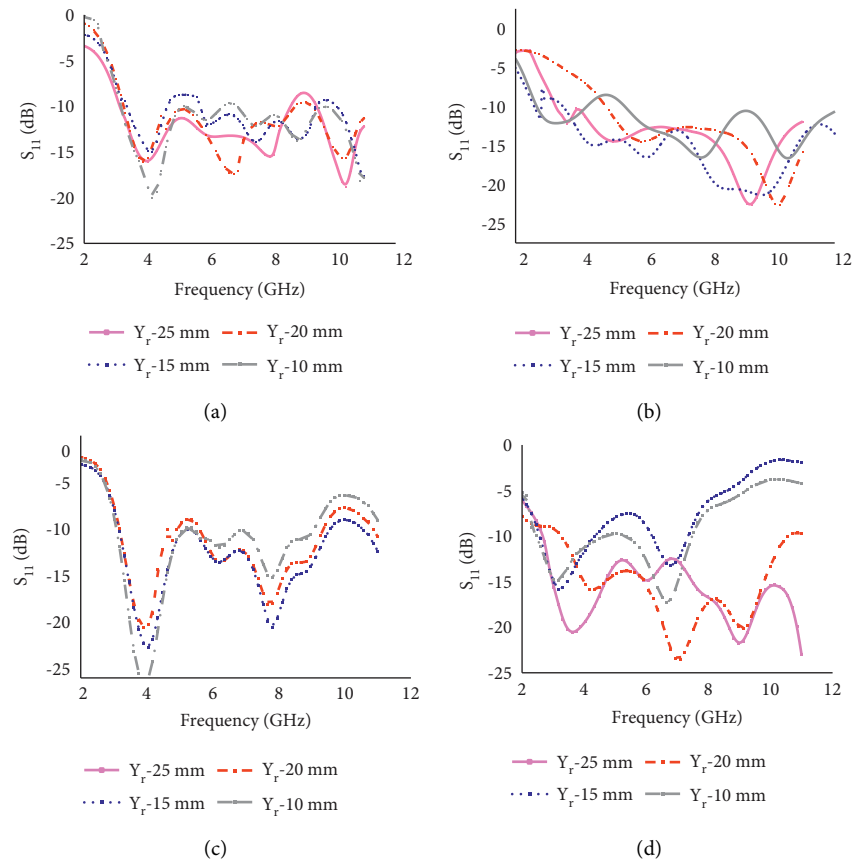


FIGURE 10: Measured reflection coefficients for different bent conditions (along the Y-direction). (a) Polyester. (b) Polyamide. (c) Denim. (d) Teslin.

photographs of the fabricated antennas and their measurements with VNA.

3.1. Reflection Coefficients. Figure 6 depicts the reflection coefficient characteristics, which represent the amount of signal reflected due to impedance discontinuity. One of the design objectives of the proposed antenna is to achieve the UWB frequency range. The four antennas achieve bandwidths ranging from 3.1 to more than 12 GHz, at the simulation level. The proposed polyester, polyamide, denim, and Teslin-based antennas have impedance bandwidths of 116% (3.1–11.7 GHz), 117% (3.13–12 GHz), 114% (3.05–11.3 GHz), and 121% (2.9–11.8 GHz), respectively. The measured response of the proposed antennas agrees reasonably well with the simulation results. However, there is a shift in the simulated and measured reflection coefficients due to manual fabrication, use of a small ground plane, and connector losses.

3.2. Radiation Characteristics. The radiation pattern is another important feature of the antenna. The radiation patterns are measured at 3.1 GHz (lowest operating frequency), 6 GHz, and 10.6 GHz (highest operating frequency) of the desired UWB range. The proposed antennas achieve bidirectional and nearly omnidirectional patterns in the E-plane and H-plane, as represented in Figure 7. Figure 8 depicts the

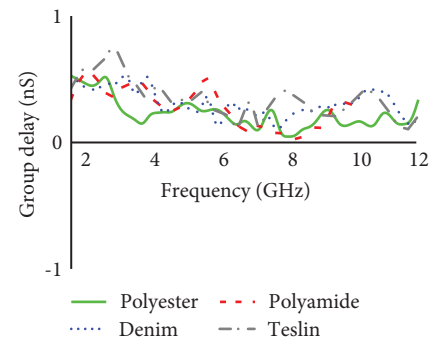


FIGURE 11: Measured group delay of the proposed antennas.

gain and efficiency values of the proposed antennas. The gain of the designed antennas is 4.3 dBi, 4.2 dBi, 4.1 dBi, and 4.1 dBi for polyester, polyamide, denim, and Teslin, respectively, and the efficiencies are 95%, 90%, 70%, and 90%.

3.3. Bending Analysis. The bending analysis is carried out to analyze the performance of the proposed antennas when they are placed on various curved surfaces of the human body [26, 27]. Figures 9 and 10 show the effect of bending along the X- and Y-directions with bent radii of 10 mm, 15 mm, 20 mm, and 25 mm. The designed flexible antennas maintain good impedance matching over the desired band at different

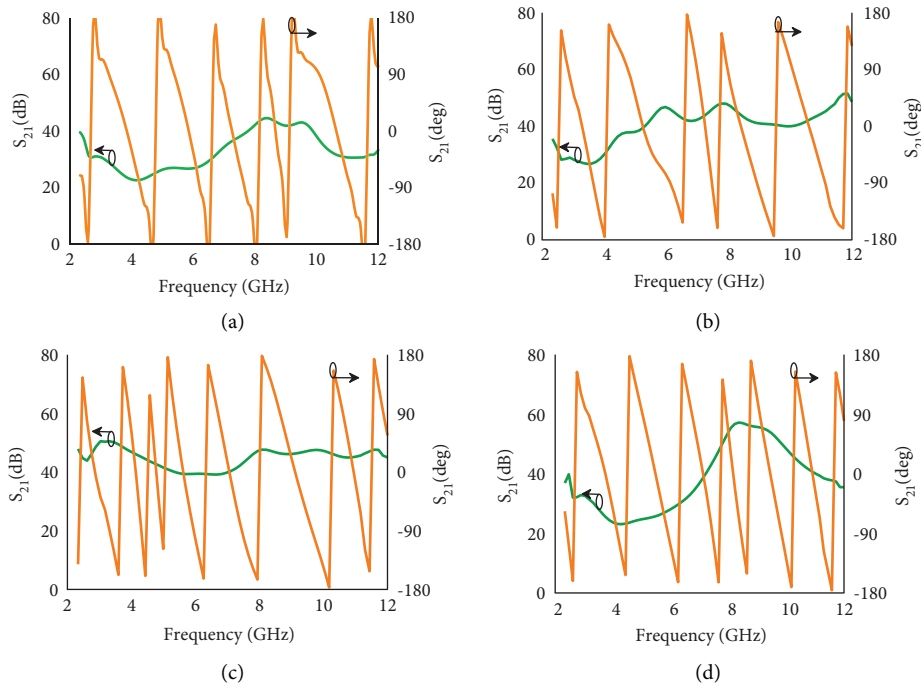


FIGURE 12: Measured phase and transmission characteristics of the proposed antennas.

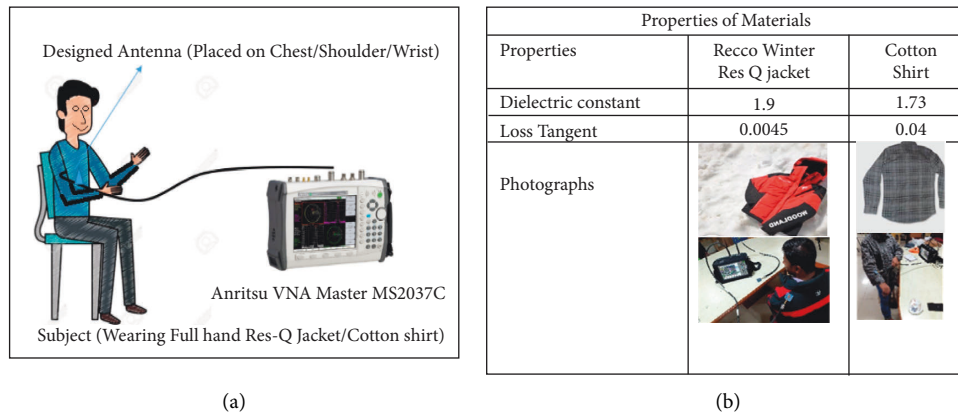


FIGURE 13: (a) Measurement setup. (b) Properties of Res-Q jacket/cotton shirt.

bending radii. However, the impedance bandwidth of Teslin paper decreases under severe bent conditions such as 15 mm and 10 mm. This performance degradation occurs due to the flexing of the thin microstrip feed line width. Also, severe bending less than 15 mm is of less importance because major parts of the human body are not conformal to that extent. Thus, the proposed antennas display negligible deterioration until a bend radius of 15 mm, covering the UWB range.

3.4. Group Delay and Transmission Characteristics. Another significant characteristic, group delay, is determined to analyze the time domain (transient) characteristics of the proposed antennas. The measured group delay of the four antennas is depicted in Figure 11. The designed antenna has group delay variations of less than 0.5 ns, indicating that the signal propagates with less distortion across the UWB

range. The phase and transmission characteristics of the proposed antennas [28, 29] are measured and represented in Figure 12. The four antennas with flexible substrates almost achieve flat S_{21} characteristics and maintain phase linearity. Thus, it confirms that the proposed antennas are well suitable for wideband systems.

3.5. On-Body Performance Analysis. The measurement setup with the Res-Q jacket/full-sleeve cotton shirt is shown in Figure 13. Figure 14 presents the reflection coefficient characteristics with the antennas placed in different locations on the body while wearing a jacket (Woodland’s Res-Q). The measurement is performed to validate the performance of the designed antennas by placing them on different parts of the human body such as the chest, wrist, and shoulder. The reflection coefficients shift slightly in the on-

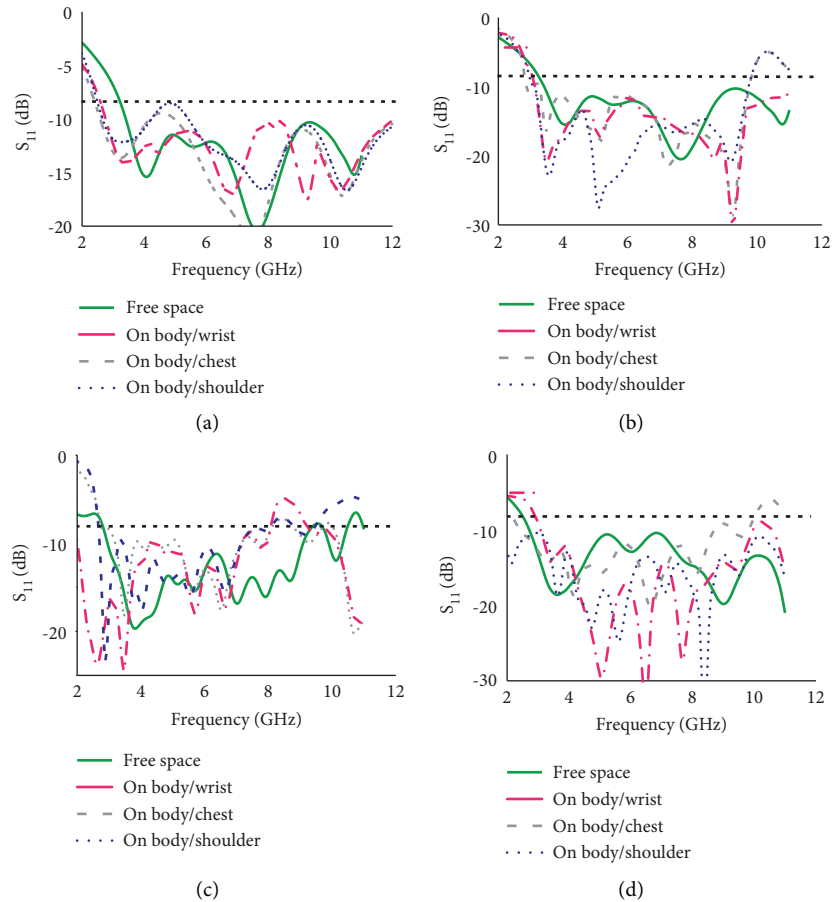


FIGURE 14: Measured reflection coefficients with the antennas placed in different locations on the body (with jacket). (a) Polyester. (b) Polyamide. (c) Denim. (d) Teslin.

body state. This frequency detuning occurs due to the high dielectric constant property of various layers of the human body.

Furthermore, in the presence of the jacket, all antennas maintain good impedance matching over the desired band of 3.1–10.6 GHz. Figure 15 depicts the reflection coefficient characteristics obtained by integrating the antennas at various locations on the cotton-based full-sleeve shirt. The impedance mismatching is observed at some frequencies, which may be due to the combined effect of the dielectric variation of the cotton shirt and the human body. It is also noted that the detuning and impedance mismatch are less for antennas tested on the wrist due to the smaller volume and mass of the human body. When compared to a cotton shirt, the impedance matching of the designed antennas integrated with the Res-Q jacket is better. Therefore, the designed antennas could be useful for body-worn applications.

3.6. Specific Absorption Rate (SAR) Analysis. The SAR analysis is important for wearable technology as electromagnetic waves emitted by the antennas are absorbed by the human body [30, 31]. The high permittivity of the body causes frequency detuning from the resonance when

the antenna is placed on the human body. The back- and side-lobe radiations are also absorbed in body tissues. Figure 16 depicts the human tissue model for SAR analysis. The SAR values are simulated by placing the four designed antennas in various locations on the human body, as shown in Table 3. The proposed antennas have a low SAR value of 0.16 W/Kg, which is much lower than the 1.6 W/Kg of the Federal Communications Commission (FCC) standards.

3.7. Path Loss Analysis. In wireless communication, the received signal strength (RSS) and corresponding path loss are important parameters to describe signal propagation/attenuation between the transmitter and receiver. In this study, the RSS of four antennas with different substrate properties is measured to determine path loss. Figure 17 depicts the measurement setup that includes an Anritsu MS2830 A signal generator (9 kHz to 6 GHz) and an Agilent signal analyzer (9 kHz to 6 GHz). A standard calibrated antenna operating at 3.5 GHz frequency is connected to the signal generator as the transmitter, and the signal analyzer and proposed antennas serve as the receiver. The measurements are taken by varying the distance between the transmitting and receiving antennas.

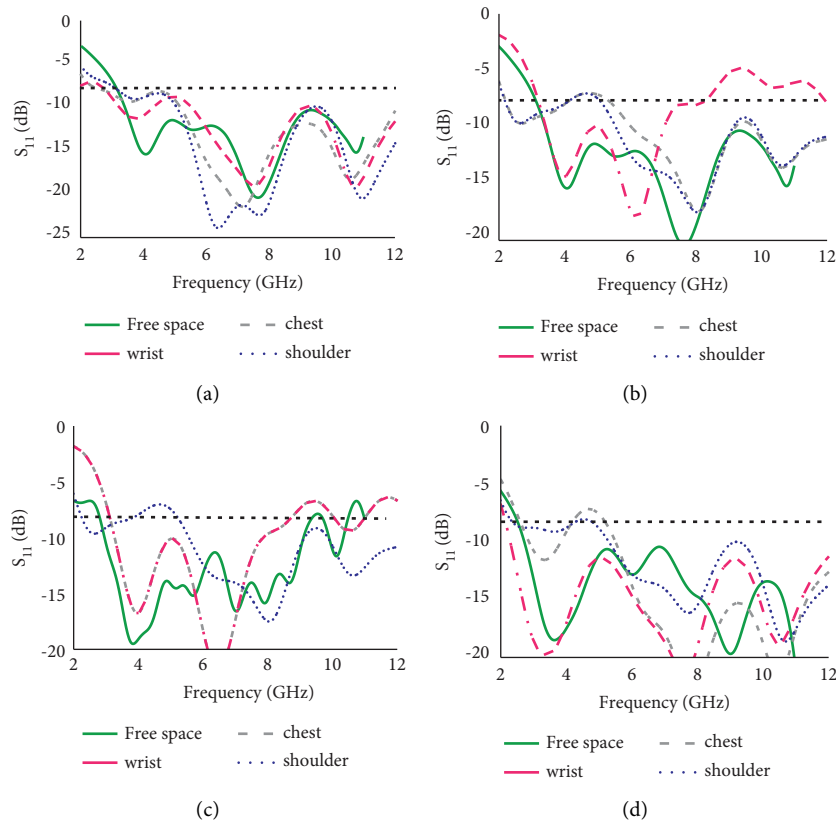


FIGURE 15: Measured reflection coefficients with the antennas placed in different locations on the body (with cotton shirt). (a) Polyester. (b) Polyamide. (c) Denim. (d) Teslin.



FIGURE 16: Human tissue model for SAR analysis.

TABLE 3: SAR values of the proposed antennas on different parts of the human body.

Different locations on the body	Proposed antenna	SAR analysis for 1 g model (W/Kg)		
		Frequency		
		3 GHz	6 GHz	10 GHz
Forehead	Polyester	0.01	0.03	0.06
Forearm		0.14	0.08	0.07
Chest		0.07	0.12	0.05
Forehead	Polyamide	0.07	0.12	0.05
Forearm		0.01	0.03	0.07
Chest		0.16	0.04	0.08
Forehead	Denim	0.06	0.10	0.04
Forearm		0.01	0.03	0.01
Chest		0.13	0.06	0.01
Forehead	Teslin	0.01	0.03	0.06
Forearm		0.15	0.08	0.05
Chest		0.07	0.11	0.07

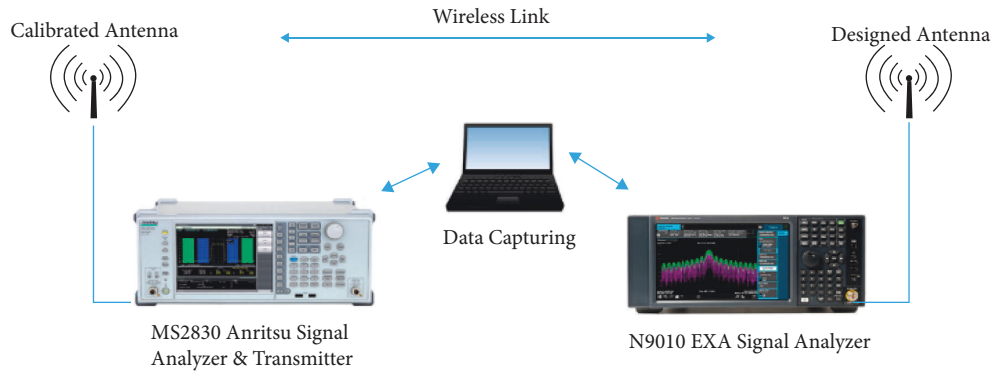


FIGURE 17: Setup for the RSS measurement.

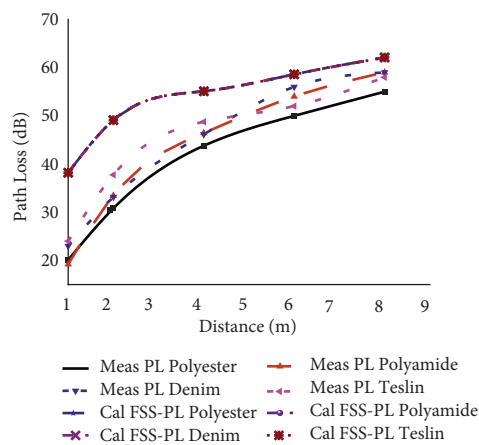


FIGURE 18: Comparison of the measured path loss with the FSPL.

TABLE 4: Comparison of the proposed antennas to previously published antenna structures.

Ref.	Antenna size (mm ²)	Substrate	Frequency range (GHz)	BW (%)	Gain (dBi)	n (%)
[13]	30 × 33	Kapton polyimide	3.1–10.6	109	—	—
[14]	48 × 35	Kapton	1–8	155	3.1	—
[15]	30 × 40	Cotton	3–12	120	3	—
[16]	52 × 37	Polyimide	1.4–16	167	>2.8	—
[17]	30 × 25	RT/duroid 5880	3.14–11.53	114	5.25	91
[23]	58 × 40	Rubber polymer	2.47	13.6	—	18.3
[27]	40 × 50	Polyamide	1.85–13.3	151	5.53	—
		Teslin	1.45–13.5	161	4.4	—
		Polyester	3.1–11.7	116	4.3	>95
This work	42 × 40	Polyamide	3.1–12.0	117	4.2	>90
		Denim	3.1–11.3	115	4.1	>60
		Teslin	2.9–11.8	121	4.1	>90

Figure 18 shows a comparison of measured path losses to free space path loss (FSPL) at 3.5 GHz. The RSS from four antennas is measured, and path loss is calculated at various distances. The graph shows that the path loss increases with frequency, and it is very low when compared to the calculated FSPL for the proposed antennas. The Teslin-based antenna has a high path loss when compared to the other three flexible substrates.

4. Salient Features of the Proposed Antenna

Table 4 compares the proposed work to previously published antenna structures. In comparison to [7, 8, 13], and [19], the proposed antennas are small in size. When compared to [8, 14], they show a wider bandwidth with a simpler design and achieve higher gain and efficiency than [7–27].

The main features of the proposed antennas are as follows:

- (i) In comparison to [7, 8, 20], the proposed antennas maintain the targeted UWB and provide a higher bandwidth percentage
- (i) In comparison to the reported antennas, the proposed antennas offer peak gains greater than 4 dBi and efficiency greater than 90% (except for a denim-based antenna)
- (ii) When compared to similar antennas (with nearly the same lower cutoff frequency/broadband nature) [7–14, 20], and [24], the proposed antennas show less SAR of 0.16 W/Kg
- (iv) The antenna prototypes exhibit less than 0.5 ns group delay variation over the operating band than [9], indicating that the proposed antennas have low phase distortion
- (v) The time domain analysis (transmission characteristics—to understand the pulse handling capability) and RSS measurements are also presented to validate the attenuation characteristics of the designed antennas, which were not reported in [7–14, 20], and [24]

The polyester substrate antenna outperforms the designed antennas. However, each substrate is intended to be used for a specific application. The polyester substrate-based antenna can be used in firefighter clothing due to its lightweight, flexibility, and ease of fabrication. The polyamide substrate is recommended for military wearables due to its flexibility, durability, heat resistance, and thermal conductivity. The denim-based antenna can be used for daily wear and medical applications as it has a higher flexibility/bending nature and lower cost. Similarly, the Teslin paper-based antenna is recommended for sports applications such as wristbands/tags due to its durability (when laminated) and versatility.

5. Conclusion

Four UWB compact flexible antennas are designed and their performances are evaluated for wearable applications. The antennas are placed close to the human body (with a high-end Res-Q jacket and cotton shirt) in order to validate their conformal nature and flexibility. The experimental results (minimal and acceptable degradation during body-worn implementation) strongly support the use of the proposed antennas for wearable devices/systems. The proposed antennas offer a bandwidth >7.5 GHz, better gain and efficiency, low SAR values, good path loss characteristics, and fewer group delay variations. The designed flexible antennas can be seamlessly integrated into the cotton outfits and are recommended for healthcare, sports, rescue, and security applications.

Data Availability

The data used to support the findings are available from the corresponding author upon request.

Conflicts of Interest

The authors declare that they have no conflicts of interest.

Acknowledgments

The authors are grateful to DRDO and DST, the Govt. of India, for supporting this work.

References

- [1] L. Corchia, G. Monti, E. De Benedetto, and L. Tarricone, "Wearable antennas for remote health care monitoring systems," *International Journal of Antennas and Propagation*, vol. 2017, p. 11, Article ID 3012341, 2017.
- [2] S. Varma, S. Sharma, M. John, R. Bharadwaj, A. Dhawan, and S. K. Koul, "Design and performance analysis of compact wearable textile antennas for IoT and body-centric communication applications," *International Journal of Antennas and Propagation*, vol. 2021, pp. 1–12, Article ID 7698765, 2021.
- [3] Ieee, "IEEE org," 2014, <https://standards.ieee.org/ieee/802.15.6/>.
- [4] G. P. Gao, C. Yang, B. Hu, R. F. Zhang, and S. F. Wang, "A wearable PIFA with an all-textile metasurface for 5 GHz WBAN applications," *IEEE Antennas and Wireless Propagation Letters*, vol. 18, no. 2, pp. 288–292, 2019.
- [5] C. Mendes and C. Peixeiro, "A dual-mode single-band wearable microstrip antenna for body Area Networks," *IEEE Antennas and Wireless Propagation Letters*, vol. 16, pp. 3055–3058, 2017.
- [6] Y. S. Chen and T. Y. Ku, "A low-profile wearable antenna using a miniature high impedance surface for smartwatch applications," *IEEE Antennas and Wireless Propagation Letters*, vol. 15, pp. 1144–1147, 2016.
- [7] S. W. Su and Y. T. Hsieh, "Integrated metal-frame antenna for smartwatch wearable device," *IEEE Transactions on Antennas and Propagation*, vol. 63, no. 7, pp. 3301–3305, July 2015.
- [8] R. Fernandez, M. A. Ilham, H. Andre, and D. Firdaus, "A wideband rectangular patch microstrip antenna using quad-slotted ground plane," *IOP Conference Series: Materials Science and Engineering*, vol. 846, no. 1, Article ID 012033, 2020.
- [9] K. Srilatha, "Progress in research," *Journal de Physique: Conf. Ser.*, vol. 180, Article ID 43543, 2021.
- [10] A. Badisa, K. Srilatha, and S. Das, "A circularly polarized quad-band wearable textile antenna integrated with triple band AMC reflector for WBAN applications," *Progress In Electromagnetics Research C*, vol. 121, pp. 1–18, 2022.
- [11] S. M. Kayser Azam, A. K. M. Zakir Hossain, M. I. Ibrahimy, and S. M. A. Motakabber, "A low-profile flexible planar monopole antenna for biomedical applications," *Engineering Science and Technology, an International Journal*, vol. 35, Article ID 101112, 2022.
- [12] B. Sugumaran and R. Balasubramanian, "Reduced specific absorption rate compact flexible monopole antenna system for smart wearable wireless communications," *Engineering Science and Technology, an International Journal*, vol. 24, no. 3, pp. 682–693, 2021.
- [13] H. R. Khaleel, "Design and fabrication of compact inkjet-printed antennas for integration within flexible and wearable electronics," *IEEE Transactions on Components, Packaging, and Manufacturing Technology*, vol. 4, no. 10, pp. 1722–1728, 2014.
- [14] Z. Hamouda, J. Wojkiewicz, A. A. Pud, L. Kone, S. Bergheul, and T. Lasri, "Flexible UWB organic antenna for wearable

- technologies application,” *IET Microwaves, Antennas & Propagation*, vol. 12, no. 2, pp. 160–166, 2018.
- [15] Y. Sun, S. W. Cheung, and T. I. Yuk, “Design of a textile ultra-wideband antenna with stable performance for body-centric wireless communications,” *IET Microwaves, Antennas & Propagation*, vol. 8, no. 15, pp. 1363–1375, 2014.
- [16] Z. Wang, L. Qin, Q. Chen, W. Yang, and H. Qu, “Flexible UWB antenna fabricated on polyimide substrate by surface modification and in situ self-metallization technique,” *Microwave Engineering*, vol. 206, pp. 12–16, 2019.
- [17] B. Prudhvi Nadh, B. T. P. Madhav, M. Siva Kumar, M. Venkateswara Rao, and T. Anilkumar, “Circular ring structured ultra-wideband antenna for wearable applications,” *International Journal of RF and Microwave Computer-Aided Engineering*, vol. 29, no. 4, p. e21580, 2019.
- [18] S. Kassim, H. A. Rahim, P. J. Soh et al., “Flexible Co-planar waveguide (CPW)-Fed Y-shaped patch UWB antenna for off-body communication,” *Journal de Physique: Conf. Ser.* vol. 1464, no. 1, p. 012058, 2020.
- [19] D. G. Mirac and C. Bulent, “Flex,” *Print. Electron*, vol. 702, p. 5002, 2022.
- [20] A. Abdu, H. X. Zheng, H. A. Jabire, and M. Wang, “CPW-fed flexible monopole antenna with H and two concentric C slots on textile substrate, backed by EBG for WBAN,” *International Journal of RF and Microwave Computer-Aided Engineering*, vol. 28, no. 7, p. e21505, 2018.
- [21] A. Alemaryeen and S. Noghianian, “AMC Integrated Textile Monopole Antenna for Wearable Applications,” *Applied Computational Electromagnetics Society Journal*, vol. 31, pp. 612–618, 2016.
- [22] B. Mandal and S. K. Parui, “Wearable tri-band SIW based antenna on leather substrate,” *Electronics Letters*, vol. 51, no. 20, pp. 1563–1564, 2015.
- [23] C. M. Lee, Y. Kim, Y. Kim, I. K. Kim, and C. W. Jung, “A flexible and transparent antenna on a polyamide substrate for laptop computers,” *Microwave and Optical Technology Letters*, vol. 57, no. 5, pp. 1038–1042, 2015.
- [24] W. El Hajj, C. Person, and J. Wiart, “A novel investigation of a broadband integrated inverted-F antenna design; application for wearable antenna,” *IEEE Transactions on Antennas and Propagation*, vol. 62, no. 7, pp. 3843–3846, 2014.
- [25] C. A. Balanis, *Antenna Theory: Analysis and Design*, John Wiley, 3rd ed edition, 2005.
- [26] S. Zahran, M. Abdalla, and A. Gaafar, *How Bending Affects a Flexible UWB Antenna*, pp. 58–63, Reaseach, China, 2017.
- [27] P. Sandeep Kumar, T. Rama Rao, N. Tiwari, and M. Balachary, “Design and analysis of wideband monopole antennas for flexible/wearable wireless device applications,” *Progress In Electromagnetics Research M*, vol. 62, pp. 167–174, 2017.
- [28] G. Quintero, J. F. Zurcher, and A. K. Skrivervik, “System fidelity factor: a new method for comparing UWB antennas,” *IEEE Transactions on Antennas and Propagation*, vol. 59, no. 7, pp. 2502–2512, 2011.
- [29] Y. Kong, Y. Li, W. Yu, and K. Yu, “A quadruple band-notched UWB antenna by using arc-shaped slot and rotated E-shaped resonator,” *Applied Computational Electromagnetics Society Journal*, vol. 31, no. 11, pp. 1316–1321, 2016.
- [30] D. Liu, T. G. Ma, and Z. Ying, “Wearable and RFID antennas,” *International Journal of Antennas and Propagation*, vol. 2013, Article ID 319306, 23 pages, 2013.
- [31] P. Capece, “Active SAR antennas: design, development, and current programs,” *International Journal of Antennas and Propagation*, vol. 200911 pages, Article ID 796064, 2009.